pharmaceutics

MDPI

Article

Immobilized Keratin HPLC Stationary Phase—A Forgotten Model of Transdermal Absorption: To What Molecular and Biological Properties Is It Relevant?

Anna Weronika Sobańska * and Elżbieta Brzezińska

Department of Analytical Chemistry, Faculty of Pharmacy, Medical University of Lodz, ul. Muszyńskiego 1, 90-151 Lodz, Poland

* Correspondence: anna.sobanska@umed.lodz.pl

Abstract: Chromatographic retention data collected on immobilized keratin (KER) or immobilized artificial membrane (IAM) stationary phases were used to predict skin permeability coefficient (log K_p) and bioconcentration factor (log *BCF*) of structurally unrelated compounds. Models of both properties contained, apart from chromatographic descriptors, calculated physico-chemical parameters. The log K_p model, containing keratin-based retention factor, has slightly better statistical parameters and is in a better agreement with experimental log K_p data than the model derived from IAM chromatography; both models are applicable primarily to non-ionized compounds.Based on the multiple linear regression (MLR) analyses conducted in this study, it was concluded that immobilized keratin chromatographic support is a moderately useful tool for skin permeability assessment.However, chromatography on immobilized keratin may also be of use for a different purpose—in studies of compounds' bioconcentration in aquatic organisms.

Keywords: biomimetic chromatography; immobilized keratin stationary phase; immobilized artificial membrane chromatography; skin permeability; bioconcentration factor

check for updates

Citation: Sobańska, A.W.; Brzezińska, E. Immobilized Keratin HPLC Stationary Phase—A Forgotten Model of Transdermal Absorption: To What Molecular and Biological Properties Is It Relevant? *Pharmaceutics* **2023**, *15*, 1172. https://doi.org/10.3390/pharmaceutics15041172

Academic Editor: Yuehong Xu

Received: 28 February 2023
Revised: 28 March 2023
Accepted: 4 April 2023
Published: 7 April 2023

Copyright: © 2023 by the authors. Licensee MDPI, Basel, Switzerland. This article is an open access article distributed under the terms and conditions of the Creative Commons Attribution (CC BY) license (https://creativecommons.org/licenses/by/4.0/).

1. Introduction

Many chemicals enter the human body through the skin. Transdermal absorption is an important route of drugs' administration, and it is also very important in the context of environmental toxicology, since undesired xenobiotics are often absorbed transdermally. The skin permeability coefficient K_p is defined according to Equation (1):

$$K_p = \frac{K_m D}{h} \quad (1)$$

where: K_m—the partition coefficient between the stratum corneum and the vehicle; D—the effective compound's diffusion coefficient through the stratum corneum; h—the diffusional pathlength.

The experimental values of skin permeability coefficients are measured in vivo (on human volunteers), ex vivo (on excised human skin), or on animal models [1], but such data are difficult to obtain due to ethical and financial problems, and the results of experiments in this area are often inconsistent due to variations in properties of different skin samples, even taken from the same human or animal.

Apart from skin absorption, an important property of compounds of environmental concern is their bioconcentration factor in aquatic organisms (*BCF*). The bioconcentration factor is the ratio of the chemical concentration in the organism (C_B) and water (C_w), accounting for the absorption via the respiratory route (e.g., gills) and skin. It is used to assess the bioaccumulation potential of compounds [2], especially in the absence of their bioaccumulation factor (*BAF*),which accounts for dietary, dermal, and respiratory exposures. According to different regulatory agencies, different criteria of bioaccumulation

apply: bioaccumulative compounds have ***BCF*** > 5000 or ***BCF*** > 2000 [3]. In the absence of ***BAF*** or ***BCF*** data, lipophilicity measured as the octanol-water partition coefficient $\boldsymbol{K}_{ow}$ is used to assess the compounds' ability to bioaccumulate; if this is the case, the log $\boldsymbol{K}_{ow}$ threshold for bioaccumulative compounds is 5 [3,4], 4.5 [5], or 3.3 [6]. Measured and estimated bioaccumulation data are also used to assign chemicals to three bioaccumulation categories: not significantly bioaccumulative (***BCF*** or ***BAF*** < 1000), bioaccumulative (***BCF*** or ***BAF*** between 1000 and 5000), and highly bioaccumulative (***BCF*** or ***BAF*** > 5000) [7].

The ethical and financial problems related to ***BCF*** determination are similar to those encountered during $\boldsymbol{K}_p$ measurements. In in vivo experiments, the need to use human volunteers or lab animals, as well as the experiment timing, are the main limitations, and, for this reason, both $\boldsymbol{K}_p$ and ***BCF*** are frequently assessed in vitro (using cell/tissue assays or non-cell models based on chromatography or electrochromatography) or in silico (calculations that can provide valuable information even without the access to compounds' samples) [8–10].

Biomimetic chromatography essentially involves the application of stationary phases, containing proteins or phospholipids, or mobile phases, including micelles or microemulsions [11–14]. The components of biomimetic chromatographic systems (stationary or mobile phases) are designed to mimic some elements or functions of biomembranes and the interactions between these components and studied molecules resemble transport and partition phenomena encountered in a living being.

Immobilized artificial membrane (IAM) chromatography, with stationary phases containing adsorbed or covalently bound phosphatidylcholine (or, more recently, sphyngomyelin) groups, is used in modern lipohilicity studies, as well as in investigations of compounds' affinity for phospholipids, related to many biological properties of solutes [15–17]. Chromatography on immobilized protein stationary phases was originally developed to separate enantiomers [18]; apart from that, some protein-based stationary phases simulate the interaction between a molecule and main plasma proteins, such as human serum albumin (HSA) [19–22] or α_1 acid glycoprotein (AGP) [21,23–25]. Retention data obtained from chromatography in biomimetic systems are used to predict ADME (absorption, distribution, metabolism, and excretion) properties of compounds in early drug discovery phases [11,26], as well as their environmental impact—mobility in soil, bioconcentration/bioaccumulation, or aquatic toxicity [27–31]. Elements of natural biomembranes, incorporated in chromatographic systems used in pharmacokinetic studies, include also cholesterol or amide moieties [32,33].

Chromatographic descriptors have been used in skin permeability studies for many years, and separation (chromatographic or electrochromatographic) techniques used in these studies are liquid chromatography (HPLC or TLC), biopartitioning micellar chromatography, micellar electrokinetic chromatography, liposome electrokinetic chromatography, and two-dimensional gas chromatography (GC × GC) [34–47].

The relationships between the IAM chromatographic retention factor ($\boldsymbol{k}_{IAM}$) and the skin permeability coefficient have been studied most frequently for small groups of compounds (n = 10 to 32), and the resulting dependencies are mostly univariate (linear or quadratic) [35,36,39,41], the exceptions being the studies in which additional variables, e.g., McGowan's characteristic volume $\boldsymbol{V}$ or the octanol-water partition coefficient log $\boldsymbol{K}_{ow}$ [33,35,36] were incorporated. In our earlier study [48] conducted for a large group of structurally unrelated compounds (n = 160), we demonstrated that log $\boldsymbol{k}_{IAM}$ accounts for ca. 46% of total log $\boldsymbol{K}_p$ variability, and the parameters whose contribution to log $\boldsymbol{K}_p$ predictions is also significant are polar surface area (***PSA***) or polarizability ($\boldsymbol{\alpha}$).

Bioconcentration of compounds in aquatic organisms can be studied in vitro using descriptors derived from HPLC chromatography on C_{18}, C_8, C_2, and phenyl-bonded silica sorbents (aromatic hydrocarbons [49]), C_{18} and cyanopropyl- and phenyl-bonded silica (aromatic hydrocarbons, alkylbenzenes, chlorinated benzenes, phthalates, nitroaromatics, phenols, and aniline [50]), and RP-18 TLC (organic sunscreens and cosmetic preservatives [51]).

More recently, the bioconcentration of compounds in aquatic organisms has been investigated using chromatography on IAM stationary phases, developed initially to mimic molecule–biomembrane interactions in ADME studies [31,52]. Earlier research pointed to the importance of additional parameters, incorporated alongside log k_{IAM}: (i) a biodegradation estimate, ***BioWin5***, calculated using the EPISuite™ software and (to a lesser extent) topological polar surface area (***TPSA***) [52]; (ii) ***TPSA***—the fraction of sp^3 carbon atoms (F_{Csp3}) and hydrogen bond donor count (#***HD***) [31].

Turowski and Kaliszan postulated that predicting skin permeability of compounds should be based on molecules' lipophilicity and interactions with keratin, which is an important constituent of the outmost layer of the epidermis [34]. An immobilized keratin-based stationary phase, developed by Turowski and Kaliszan, was initially proposed to be an in vitro tool in investigations of solutes' skin permeability (log K_p) [34]. However, it was discovered that the retention factor obtained on this sorbent (log k_{KER}) is not a sufficiently good predictor of skin permeability coefficient, and it cannot be used as a sole descriptor in log K_p models. Turowski and Kaliszan reported that this descriptor can be combined with the chromatographic retention factor obtained by immobilized artificial membrane chromatography (log k_{IAM}), and the results of log K_p predictions using multiple linear regression (MLR) models satisfy (Equation (2)):

$$\log K_p = -6.56 + 1.92 \log k_{IAM} - 1.04 \log k_{KER} \ (n = 17, R^2 = 0.86) \quad (2)$$

Turowski and Kaliszan concluded that skin permeability increases with the lipophilicity of solutes (encoded primarily by log k_{IAM}) and decreases with their affinity for keratin (expressed as log k_{KER}). Unfortunately, the model they proposed (Equation (2)) requires two sets of chromatographic data, obtained on different stationary phases, this being the likely reason why the immobilized keratin stationary phase they proposed has never become widely popular and, to the best of our knowledge, it is not commercially available.

In this study, a novel application of immobilized keratin stationary phases developed by Turowski and Kaliszan is proposed, and chromatography on immobilized keratin sorbent is used to model compounds' bioconcentration in aquatic organisms.

2. Materials and Methods

2.1. IAM and Immobilized Keratin Chromatography

The chromatographic retention factors for the compounds analyzed in this study (Table 1) were taken from [34]. They were obtained on: (i) an IAM.PC.MG HPLC column purchased from Regis (150 × 4.6 mm, particle diameter 12 µm, pore diameter 300 Å) with a phosphate buffer (pH 6.0), including acetonitrile (95:5 *v*/*v*) mobile phase (flow rate—1 mL min^{-1}); (ii) physically immobilized keratin sorbent with pH 4.2 phosphate buffer as a mobile phase (column dimensions—125 × 4 mm; flow rate—1 mL min^{-1}). The mobile phase used in keratin chromatography (pH 4.2 buffer) was selected on the basis of QSRR studies as giving the "best" relationship between log k_{KER} and structural descriptors (molecular weight and dipole moment) [34].

2.2. Calculated Molecular Descriptors

Molecular weight (M_w), heavy atom count (#***HvAt***), aromatic heavy atom count (#***ArHvAt***), fraction of sp^3 carbons (F_{Csp3}), rotatable bond count (#***FRB***), hydrogen donor count (#***HD***), hydrogen acceptor count (#***HA***), molecular refractivity (***MR***), aqueous solubility (log ***S***), and topological polar surface area (***TPSA***) were calculated using Swiss ADME software available freely on-line [53]. The octanol–water partition coefficient (log K_{ow}) was predicted using EpiSuite [54]. Total counts of nitrogen and oxygen atoms (***N*** + ***O***) were calculated manually on the basis of compounds' molecular formulas (Table 1).

Table 1. Chromatographic retention factors and calculated physico-chemical properties of compounds **1** to **32**.

No.	Compound	log k_{KER}	log k_{IAM}	M_w	#*HvAt*	#*ArHvAt*	F_{Csp3}	#*FRB*	#*HA*	#*HD*	*MR*	*TPSA*	(*N* + *O*)	log K_{ow}	log *S*
1	2-Cresole	−0.18	0.36	108.1	8	6	0.14	0	1	1	33.4	20.2	1	1.95	−2.29
2	2-Naphtol	0.88	1.25	144.2	11	10	0	0	1	1	46.0	20.2	1	2.70	−3.11
3	3-Cresole	−0.22	0.36	108.1	8	6	0.14	0	1	1	33.4	20.2	1	1.96	−2.30
4	3-Nitrophenol	0.24	0.60	139.1	10	6	0	1	3	1	37.3	66.1	4	2.00	−2.34
5	4-Bromophenol	0.34	1.00	173.0	8	6	0	0	1	1	36.2	20.2	1	2.59	−3.10
6	4-Chlorophenol	0.27	0.73	128.6	8	6	0	0	1	1	33.5	20.2	1	2.39	−2.70
7	4-Cresole	−0.08	0.42	108.1	8	6	0.14	0	1	1	33.4	20.2	1	1.94	−2.29
8	4-Ethylphenol	−0.25	0.76	122.2	9	6	0.25	1	1	1	38.2	20.2	1	2.58	−2.65
9	4-Nitrophenol	0.19	0.60	139.1	10	6	0	1	3	1	37.3	66.1	4	1.91	−2.28
10	Baclofen	−0.33	−0.73	213.7	14	6	0.3	4	3	2	55.3	63.3	3	−0.96	−0.61
11	Chlorocresole	0.68	1.18	142.6	9	6	0.14	0	1	1	38.4	20.2	1	2.70	−3.09
12	Methylparaben	0.04	0.52	152.2	11	6	0.12	2	3	1	39.7	46.5	3	1.96	−2.29
13	Phenol	−0.27	0.37	94.1	7	6	0	0	1	1	28.5	20.2	1	1.46	−1.98
14	Phenylalanine	−0.20	−0.65	165.2	12	6	0.22	3	3	2	45.5	63.3	3	−1.44	−0.08
15	Resorcinol	−0.38	−0.14	110.1	8	6	0	0	2	2	30.5	40.5	2	0.80	−1.58
16	Salcylic acid	−0.06	−0.58	138.1	10	6	0	1	3	2	35.4	57.5	3	2.26	−2.50
17	Thymol	0.52	1.34	150.2	11	6	0.4	1	1	1	48.0	20.2	1	3.30	−3.19
18	1,2,3-tris(1-methylethyl)benzene	0.75	2.43	204.4	15	6	0.6	3	0	0	70.2	0.0	0	6.36	−4.54
19	1,4-dinitrobenzene	0.45	0.16	168.1	12	6	0	2	4	0	44.1	91.6	6	1.46	−2.04
20	3-(trifluoromethyl)phenol	0.19	1.23	162.1	11	6	0.14	1	4	1	33.5	20.2	1	2.95	−3.04
21	4-cyanophenol	−0.05	0.77	119.1	9	6	0	0	2	1	33.2	44.0	2	1.60	−2.08
22	4-iodophenol	0.80	1.59	220.0	8	6	0	0	1	1	41.2	20.2	1	2.91	−3.59
23	4-nitrobenzoic acid	−0.23	−0.23	167.1	12	6	0	2	4	1	42.2	83.1	5	1.89	−2.30
24	Anizole	−0.09	0.31	108.1	8	6	0.14	1	1	0	32.9	9.2	1	2.11	−2.33
25	Benzamide	−0.04	−0.10	121.1	9	6	0	1	1	1	34.5	43.1	2	0.64	−1.42
26	benzene	−0.27	0.09	78.1	6	6	0	0	0	0	26.4	0.0	0	2.13	−2.41
27	benzoic acid	−0.21	−0.74	122.1	9	6	0	1	2	1	33.4	37.3	2	1.87	−2.20
28	Benzonitrile	0.02	0.15	103.1	8	6	0	0	1	0	31.2	23.8	1	1.56	−2.02
29	caffeine	0.08	−0.40	194.2	14	9	0.38	0	3	0	52.0	61.8	6	−0.07	−1.48
30	Chlorobenzene	0.13	0.66	112.6	7	6	0	0	0	0	31.5	0.0	0	2.84	−2.96
31	Indazole	0.23	0.71	118.1	9	9	0	0	1	1	36.1	28.7	2	1.77	−2.72
32	Toluene	−0.05	0.44	92.1	7	6	0.14	0	0	0	31.4	0.0	0	2.73	−2.77

2.3. Reference Values of Skin Permeability Coefficient (log K_p*) and Bioconcentration Factor (log* ***BCF****)*

The experimentally determined values of log K_p and log ***BCF*** are available for only some compounds within the studied group. For this reason, the models of skin permeability and bioconcentration factor, involving chromatographic and calculated descriptors, were generated and validated using log K_p and log ***BCF*** values obtained in silico with the EpiSuite v. 4.1 software (log K_p^{EPI}—DERMWIN v. 2.02 and log BCF_{EPI}—BCFBAF v. 3.02 modules, respectively), recommended by the US Environmental Protection Agency [54,55] and tested on sub-groups of solutes whose experimental log K_p or log ***BCF*** values are known (log K_p^{exp}, log BCF_{exp}) [56,57]. The estimation methodology used by DERMWIN is based on an algorithm developed by Potts [58], and the estimations provided by BCFBAF are based on methodology developed by Meylan [59] and Arnot and Gobas [3]. The values of log K_p^{EPI} and log BCF_{EPI} obtained using EpiSuite are given in Tables 2 and 3.

Table 2. Reference (EPI), predicted, and experimental values of log K_p.

	log K_p^{EPI}	Equation (6)	Equation (7)	Equation (8)	Equation (9)	log K_p^{exp}
2-Cresole	−5.58	−5.71	−5.67	−5.89	−5.57	−5.36
2-Naphtol	−5.26	−4.99	−5.00	−5.05	−5.26	−4.76
3-Cresole	−5.57	−5.71	−5.75	−5.89	−5.65	−5.37
3-Nitrophenol	−5.73	−6.22	−6.06	−6.01	−5.98	−5.81
4-Bromophenol	−5.52	−5.20	−5.74	−5.30	−5.74	−5.00
4-Chlorophenol	−5.39	−5.42	−5.18	−5.55	−5.09	−5.00
4-Cresole	−5.58	−5.67	−5.50	−5.84	−5.39	−5.31
4-Ethylphenol	−5.21	−5.39	−5.88	−5.52	−5.80	−5.01
4-Nitrophenol	−5.79	−6.22	−6.15	−6.01	−6.08	−5.81
Baclofen	−8.28	−7.25	−7.66	−7.23	−7.69	
Chlorocresole	−5.05	−5.05	−4.53	−5.12	−4.43	−4.82
Methylparaben	−5.84	−5.98	−6.09	−5.94	−6.02	−5.63
Phenol	−5.84	−5.71	−5.76	−5.89	−5.65	−5.61
Resorcinol	−6.40	−6.43	−6.48	−6.52	−6.40	−6.63
Thymol	−4.87	−4.92	−4.66	−4.97	−4.56	−4.77

Table 2. *Cont.*

	log K_p ^{EPI}	Equation (6)	Equation (7)	Equation (8)	Equation (9)	log K_p ^{exp}
1,2,3-tris(1-methylethyl)benzene	−3.78	−3.73	−4.13	−3.80	−4.06	
1,4-dinitrobenzene	−6.29	−6.96	−6.38	−6.61	−6.32	
3-(trifluoromethyl)phenol	−5.19	−5.01	−5.44	−5.07	−5.38	
4-cyanophenol	−5.89	−5.74	−5.96	−5.68	−5.86	−5.73
4-iodophenol	−5.58	−4.71	−5.64	−4.74	−5.70	
Anizole	−5.46	−5.59	−5.29	−5.86	−5.18	
Benzamide	−6.58	−6.43	−5.96	−6.50	−5.86	
Benzene	−5.26	−5.63	−5.22	−6.00	−5.09	−4.51
Benzonitrile	−5.82	−5.94	−5.31	−6.12	−5.19	
Caffeine	−7.53	−6.96	−7.38	−6.91	−7.66	−7.56
Chlorobenzene	−4.97	−5.17	−4.92	−5.47	−4.81	
Indazole	−5.44	−5.56	−5.94	−5.63	−6.11	
Toluene	−4.92	−5.35	−4.92	−5.68	−4.78	−3.64

Table 3. Reference, predicted, and experimental values of log ***BCF***.

	log BCF_{EPI}	Equation (10)	Equation (11)	Equation (12)	Equation (13)	log BCF_{exp}
2-Cresole	0.95	1.13	0.97	1.01	0.98	1.03
2-Naphtol	1.45	1.47	1.48	1.43	1.45	
3-Cresole	0.96	1.13	0.94	1.01	0.94	1.23
3-Nitrophenol	0.99	0.85	0.64	0.98	0.67	
4-Bromophenol	1.38	1.31	1.44	1.23	1.52	1.17
4-Chlorophenol	1.24	1.14	1.29	1.03	1.37	1.42
4-Cresole	0.95	1.17	1.04	1.06	1.06	
4-Ethylphenol	1.37	1.55	1.11	1.52	1.10	
4-Nitrophenol	0.93	0.85	0.60	0.98	0.63	0.71
Baclofen	0.50	0.51	0.99	0.53	0.90	
Chlorocresole	1.45	1.64	1.77	1.63	1.90	
Methylparaben	0.96	1.08	0.93	1.12	0.94	
Phenol	0.63	0.92	0.71	0.76	0.71	
Phenylalanine	0.50	0.44	0.70	0.44	0.65	
Resorcinol	0.50	0.51	0.37	0.40	0.34	
Salcylic acid	0.50	0.17	0.50	0.09	0.50	
Thymol	1.84	2.13	2.03	2.23	2.12	1.48
1,2,3-tris(1-methylethyl)benzene	3.86	3.20	3.41	3.40	3.49	
1,4-dinitrobenzene	0.63	0.46	0.62	0.67	0.65	
3-(trifluoromethyl)phenol	1.61	1.67	1.23	1.67	1.30	
4-cyanophenol	0.72	1.06	0.65	1.09	0.66	0.91
4-iodophenol	1.59	1.67	1.96	1.68	2.10	
4-nitrobenzoic acid	0.50	0.27	0.21	0.37	0.15	
Anizole	1.06	1.15	1.20	0.96	1.23	
Benzamide	0.50	0.53	0.72	0.43	0.73	
Benzene	1.07	0.84	0.98	0.53	1.00	
Benzoic acid	0.50	0.16	0.66	−0.06	0.65	0.93
Benzonitrile	0.70	0.77	0.96	0.60	1.00	
Caffeine	0.50	0.84	0.63	0.93	0.48	
Chlorobenzene	1.54	1.19	1.45	0.95	1.52	1.34
Indazole	0.83	1.09	0.67	1.03	0.61	
Toluene	1.47	1.27	1.33	1.05	1.37	1.02

2.4. Statistical Tools

Multiple linear regression (MLR) models were generated using Statistica v. 13 by StatSoft Polska, Kraków, Poland, and this refers to the stepwise forward regression mode.

The models considered in this study were evaluated using the following procedures:

- Cross-validation was performed, with n compounds from the initial training set split into 2 subsets, one of which was used to train a new model and the remaining one to test it. After cross-validation, the RMSEP (root mean squared error of prediction) for the particular N-compound test subset was calculated as follows (Equation (3)):

$$RMSEP = \sqrt{\frac{\sum_{i=1}^{N}\left(y_i^{pred} - y_i^{ref}\right)^2}{N}} \quad (3)$$

- Comparison of the predicted log $\boldsymbol{K}_p{}^{pred}$ and log $\boldsymbol{BCF}_{pred}$ values (calculated for the compounds, whose experimental log $\boldsymbol{K}_p{}^{exp}$ and log $\boldsymbol{BCF}_{exp}$ data are available) was per-

formed, and these data were analyzed using the squared coefficient of determination (R^2_{exp}).

3. Results

3.1. Keratin vs. IAM HPLC Skin Permeability Models

In this study, we compared the log $\boldsymbol{K}_p$ models obtained using log $\boldsymbol{k}_{IAM}$ and ***TPSA*** (Equation (4)) with the models including log $\boldsymbol{k}_{KER}$ as a chromatographic parameter (Equation (5)).

$$\log \boldsymbol{K}_p = -5.61\ (\pm 0.24) + 0.68\ (\pm 0.17) \log \boldsymbol{k}_{IAM} - 0.014\ (\pm 0.005)\ \boldsymbol{TPSA}$$
$$(n = 32,\ R^2 = 0.63,\ R^2_{adj.} = 0.63,\ R^2_{exp} = 0.72,\ F = 25.1,\ p < 0.01) \quad (4)$$

$$\log \boldsymbol{K}_p = -2.56\ (\pm 0.83) + 1.74\ (\pm 0.38) \log \boldsymbol{k}_{KER} - 0.011\ (\pm 0.008)\ \boldsymbol{M}_w$$
$$- 0.22\ (\pm 0.11)\ \boldsymbol{\#ArHvAt} - 0.014\ (\pm 0.005)\ \boldsymbol{TPSA}$$
$$(n = 32,\ R^2 = 0.68,\ R^2_{adj.} = 0.63,\ R^2_{exp} = 0.73,\ F = 14.3,\ p < 0.01) \quad (5)$$

It was observed that neither Equation (4), nor (5), gives satisfying results of log $\boldsymbol{K}_p$ predictions for relatively strongly ionized solutes (compounds **14**, **16**, **23**, and **27**); when these compounds were excluded from the analysis, Equations (6) and (7) were obtained for a group of 28 neutral, basic, or weakly acidic compounds (Figures 1 and 2, Table 2).

$$\log \boldsymbol{K}_p = -5.70 + 0.81\ (\pm 0.17) \log \boldsymbol{k}_{IAM} - 0.015\ (\pm 0.004)\ \boldsymbol{TPSA}$$
$$(n = 28,\ R^2 = 0.80,\ R^2_{adj.} = 0.78,\ R^2_{exp} = 0.73,\ F = 49.7,\ p < 0.01) \quad (6)$$

$$\log \boldsymbol{K}_p = -2.73\ (\pm 0.54) + 1.80\ (\pm 0.26) \log \boldsymbol{k}_{KER} - 0.015\ (\pm 0.003)\ \boldsymbol{M}_w + 0.13\ (\pm 0.05)\ \boldsymbol{\#HvAt} - 0.27\ (\pm 0.07)$$
$$\boldsymbol{\#ArHvAt} - 0.020\ (\pm 0.004)\ \boldsymbol{TPSA}$$
$$(n = 28,\ R^2 = 0.85,\ R^2_{adj.} = 0.81,\ R^2_{exp} = 0.79,\ F = 24.8,\ p < 0.01) \quad (7)$$

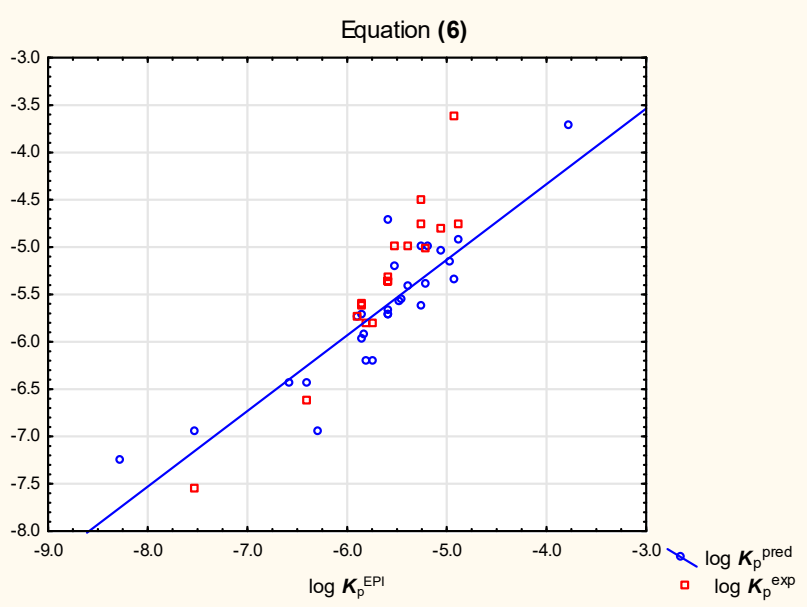

Figure 1. Equation (6)—predicted and experimental log $\boldsymbol{K}_p$ vs. reference values.

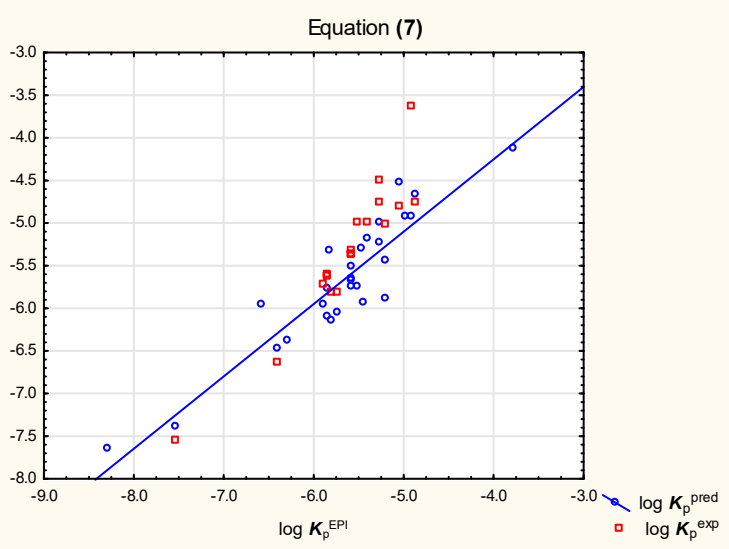

Figure 2. Equation (7)—predicted and experimental log $\boldsymbol{K}_p$ vs. reference values.

The likely reason for such discrepancies between the predicted (Equations (4) and (5)) and reference values of log $\boldsymbol{K}_p$ for relatively strongly ionizable compounds is that the reference model has also its limitations: it overestimates the results for very hydrophilic molecules, underestimates the values for non-hydrogen bonding solutes, and fails for extremely lipophilic compounds or solutes having a very high tendency to hydrogen bonding [60–62].

At this point, the group of 28 studied compounds was divided into two subsets: a training set (**1** to **20**) and a test set (**21** to **28**). Equations (8) and (9) generated for the training set, and containing the same sets of independent variables as Equations (6) and (7), are as follows (Table 2):

$$\log \boldsymbol{K}_p = -6.09\ (\pm 0.27) + 0.94\ (\pm 0.17) \log \boldsymbol{k}_{IAM} - 0.0073\ (\pm 0.005)\ \boldsymbol{TPSA}$$
$$(n = 20,\ R^2 = 0.80,\ R^2_{adj.} = 0.78,\ RMSEP = 0.51,\ F = 34.2,\ p < 0.01) \quad (8)$$

$$\log \boldsymbol{K}_p = -1.93\ (\pm 0.54) + 1.85\ (\pm 0.28) \log \boldsymbol{k}_{KER} - 0.017\ (\pm 0.003)\ \boldsymbol{M}_w + 0.15\ (\pm 0.05)\ \boldsymbol{\#HvAt} - 0.37\ (\pm 0.11)\ \boldsymbol{\#ArHvAt} - 0.021\ (\pm 0.004)\ \boldsymbol{TPSA}$$
$$(n = 20,\ R^2 = 0.87,\ R^2_{adj.} = 0.83,\ RMSEP = 0.44,\ F = 19.0,\ p < 0.01) \quad (9)$$

3.2. Keratin HPLC Models of Bioconcentration Factor

According to our earlier research, the bioconcentration factor log ***BCF*** can be predicted using log $\boldsymbol{k}_{IAM}$ and two additional parameters: $\boldsymbol{F}_{Csp3}$ and ***TPSA*** [31]. The predictive potential of Equation (10) (Figure 3) is compared to that of a model based on chromatographic retention factors obtained using immobilized keratine as a stationary phase (Equation (11), Figure 4).

$$\log \boldsymbol{BCF} = 0.79\ (\pm 0.11) + 0.62\ (\pm 0.07) \log \boldsymbol{k}_{IAM} + 1.53\ (\pm 0.31)\ \boldsymbol{F}_{Csp3} - 0.0046\ (\pm 0.0021)\ \boldsymbol{TPSA}$$
$$(n = 32,\ R^2 = 0.87,\ R^2_{adj.} = 0.86,\ R^2_{exp} = 0.41,\ F = 63.9,\ p < 0.01) \quad (10)$$

$$\log \boldsymbol{BCF} = 1.23\ (\pm 0.34) + 0.70\ (\pm 0.15) \log \boldsymbol{k}_{KER} - 0.18\ (\pm 0.05)\ \boldsymbol{\#ArHvAt} + 0.039\ (\pm 0.006)\ \boldsymbol{MR} - 0.017\ (\pm 0.002)\ \boldsymbol{TPSA}$$
$$(n = 32,\ R^2 = 0.88,\ R^2_{adj.} = 0.86,\ R^2_{exp} = 0.69,\ F = 50.3,\ p < 0.01) \quad (11)$$

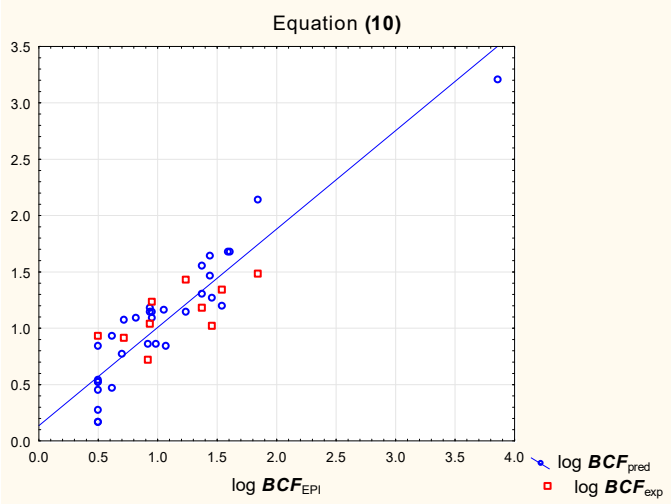

Figure 3. Equation (10)—predicted and experimental log ***BCF*** vs. reference values.

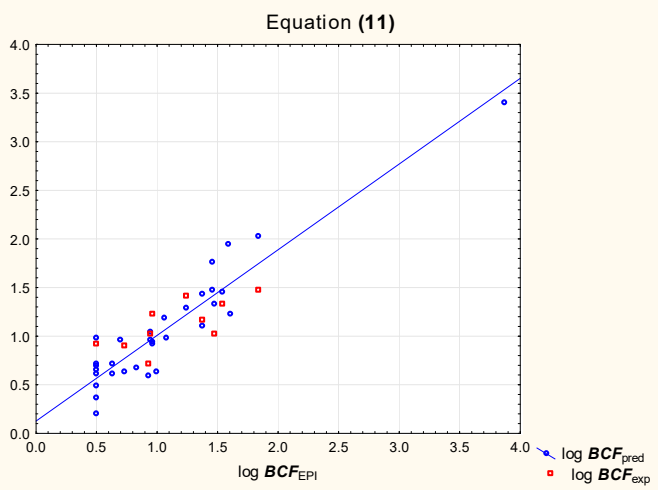

Figure 4. Equation (11)—predicted and experimental log ***BCF*** vs. reference values.

At this point, the group of 32 studied compounds was divided into two subsets: a training set (**1** to **20**) and a test set (**21** to **32**). Equations (12) and (13) generated for the training set, and containing the same sets of independent variables as Equations (10) and (11) are as follows:

$$\log \boldsymbol{BCF} = 0.46\ (\pm 0.15) + 0.75\ (\pm 0.09) \log \boldsymbol{k}_{\mathrm{IAM}} + 1.84\ (\pm 0.34)\ \boldsymbol{F}_{\mathrm{Csp3}} + 0.0010\ (\pm 0.0028)\ \boldsymbol{TPSA} \quad (12)$$
$$(n = 20,\ R^2 = 0.93,\ R^2_{\mathrm{adj.}} = 0.92,\ \mathrm{RMSEP} = 0.36,\ F = 72.2,\ p < 0.01)$$

$$\log \boldsymbol{BCF} = 1.59\ (\pm 0.57) + 0.85\ (\pm 0.20) \log \boldsymbol{k}_{\mathrm{KER}} - 0.22\ (\pm 0.08)\ \boldsymbol{\#ArHvAt} + 0.037\ (\pm 0.007)\ \boldsymbol{MR} - 0.018\ (\pm 0.003)\ \boldsymbol{TPSA} \quad (13)$$
$$(n = 20,\ R^2 = 0.90,\ R^2_{\mathrm{adj.}} = 0.88,\ \mathrm{RMSEP} = 0.23,\ F = 35.1,\ p < 0.01)$$

4. Discussion

In our study, we investigated the possibility of using log $\boldsymbol{k}_{\mathrm{KER}}$ in skin permeability models, alongside additional descriptors that were either not considered or not available when the keratin stationary phase was originally developed. We studied correlations between log $\boldsymbol{k}_{\mathrm{KER}}$ and the key physico-chemical properties associated with compounds' ability to cross biological barriers (Table 4) and discovered that log $\boldsymbol{k}_{\mathrm{KER}}$ encodes primarily

lipophilicity (log K_{ow}) and aqueous solubility (log ***S***), which are important factors governing the ability of compounds to cross the skin barrier, but the correlations are moderate.

Table 4. Correlations ® between chromatographic and calculated parameters (n= 32).

	log k_{KER}	**log k_{IAM}**	***M_w***	***#HvAt***	***#ArHvAt***	***F_{Csp3}***	***#FRB***	***#HA***	***#HD***	***MR***	***TPSA***	**log K_{ow}**	**log *S***
log k_{KER}	1.00	0.75	0.48	0.26	0.33	0.15	−0.07	−0.15	−0.25	0.45	−0.16	0.57	−0.67
log k_{IAM}	**0.75**	1.00	0.20	0.00	0.06	0.26	−0.19	−0.42	−0.31	0.26	−0.54	0.81	−0.85
M_w	0.48	0.20	1.00	0.77	0.12	0.43	0.57	0.43	0.18	0.80	0.39	0.01	−0.09
#HvAt	0.26	0.00	0.77	1.00	0.25	0.62	0.75	0.56	0.13	0.89	0.54	−0.08	0.11
#ArHvAt	0.33	0.06	0.12	0.25	1.00	0.03	−0.24	−0.02	−0.09	0.24	0.02	−0.09	−0.05
F_{Csp3}	0.15	0.26	0.43	0.62	0.03	1.00	0.46	−0.09	−0.12	0.75	−0.16	0.21	−0.13
#FRB	−0.07	−0.19	0.57	0.75	−0.24	0.46	1.00	0.49	0.25	0.66	0.48	−0.18	0.30
#HA	−0.15	−0.42	0.43	0.56	−0.02	−0.09	0.49	1.00	0.38	0.18	0.87	−0.45	0.45
#HD	−0.25	−0.31	0.18	0.13	−0.09	−0.12	0.25	0.38	1.00	0.00	0.37	−0.42	0.40
MR	0.45	0.26	0.80	0.89	0.24	0.75	0.66	0.18	0.00	1.00	0.23	0.16	−0.14
TPSA	−0.16	−0.54	0.39	0.54	0.02	−0.16	0.48	0.87	0.37	0.23	1.00	−0.57	0.57
log K_{ow}	**0.57**	0.81	0.01	−0.08	−0.09	0.21	−0.18	−0.45	−0.42	0.16	−0.57	1.00	−0.96
log ***S***	**−0.67**	−0.85	−0.09	0.11	−0.05	−0.13	0.30	0.45	0.40	−0.14	0.57	−0.96	1.00

Predictive models of log $\boldsymbol{K}_p$, involving retention parameters obtained on immobilized keratin (Equations (7) and (9)), have similar (or, in fact, slightly better) statistical parameters compared to those reported for models based on IAM chromatography (Equations (6) and (8)). Log $\boldsymbol{K}_p$ values predicted using Equation (7) are in a slightly closer agreement with experimental log $\boldsymbol{K}_p^{exp}$ data available for a subset of 18 compounds than those calculated using Equation (6). It must be noted, however, that, in the process of descriptors' selection by forward stepwise regression, chromatographic parameters log $\boldsymbol{k}_{KER}$ and log $\boldsymbol{k}_{IAM}$ behave differently. Log $\boldsymbol{k}_{IAM}$ (Equation (6)) is selected first, and it accounts for ca. 66% of total log $\boldsymbol{K}_p$ variability; log $\boldsymbol{k}_{KER}$ (Equation (7)) is selected second (after ***TPSA***), and it accounts for just 16% of total log $\boldsymbol{K}_p$ variability.

The significance of log $\boldsymbol{k}_{KER}$ as an independent variable is much higher in models of bioconcentration factor log ***BCF***. In Equation (11), log $\boldsymbol{k}_{KER}$ is the most important independent variable, accounting for 39% of total log $\boldsymbol{K}_p$ variability; further variables (selected as follows: ***TPSA***, ***MR,*** and ***#ArHvAt***) account for 24, 18, and 7% of total log $\boldsymbol{K}_p$ variability, respectively. In the IAM chromatography-based model of log ***BCF*** (Equation (10)), log $\boldsymbol{k}_{IAM}$ accounts for 73%, and other independent variables ($\boldsymbol{F}_{Csp3}$ and ***TPSA***) account for 12 and 2% of total log $\boldsymbol{K}_p$ variability, respectively. The keratin chromatographic retention-based model (11) has statistical parameters similar to those of Equation (10), derived from IAM chromatography; however, Equation (11) seems to fit the experimental data (log $\boldsymbol{BCF}_{exp}$) reported for a subset of 10 compounds better than Equation (10).

5. Conclusions

Immobilized keratine-based chromatographic stationary phase was developed in the late 1990s to help in in vitro investigations of compounds' transdermal absorption. A new model of a skin permeability coefficient was developed in the current study, which involves the chromatographic retention factor measured on the immobilized keratine sorbent (log $\boldsymbol{k}_{KER}$) and four additional independent variables (Equation (7)). This model has slightly better statistical parameters and is in a better agreement with experimental log $\boldsymbol{K}_p$ data than the model derived from IAM chromatography (Equation (6)); both models are applicable primarily to non-ionized compounds (with carboxylic acids removed from Equations (4) and (5)). Based on the MLR analyses conducted in this study, it was concluded that immobilized keratin chromatographic support is a moderately useful tool for skin permeability assessment. However, similarly to IAM chromatography in the past, chromatography on immobilized keratin may serve a different purpose; designed for applications in pharmacokinetic studies, it may also be of use in the realm of environmental science, in studies of compounds' bioconcentrations in aquatic organisms.

Author Contributions: Conceptualization, A.W.S.; methodology, A.W.S. and E.B.; investigation, A.W.S.; writing—original draft preparation, A.W.S. All authors have read and agreed to the published version of the manuscript.

Funding: This research study was supported by an internal grant of the Medical University of Lodz, no. 503/3-016-03/503-31-001.

Institutional Review Board Statement: Not applicable.

Informed Consent Statement: Not applicable.

Data Availability Statement: Data generated in this study can be found in this manuscript.

Conflicts of Interest: The authors declare no conflict of interest.

References

1. Todo, H. Transdermal Permeation of Drugs in Various Animal Species. *Pharmaceutics* **2017**, *9*, 33. [CrossRef] [PubMed]
2. Weisbrod, A.V.; Burkhard, L.P.; Arnot, J.; Mekenyan, O.; Howard, P.H.; Russom, C.; Boethling, R.; Sakuratani, Y.; Traas, T.; Bridges, T.; et al. Workgroup Report: Review of Fish Bioaccumulation Databases Used to Identify Persistent, Bioaccumulative, Toxic Substances. *Environ. Health Perspect* **2007**, *115*, 255–261. [CrossRef] [PubMed]
3. Arnot, J.A.; Gobas, F.A. A Review of Bioconcentration Factor (BCF) and Bioaccumulation Factor (BAF) Assessments for Organic Chemicals in Aquatic Organisms. *Environ. Rev.* **2006**, *14*, 257–297. [CrossRef]
4. Arnot, J.A.; Gobas, F.A.P.C. A Generic QSAR for Assessing the Bioaccumulation Potential of Organic Chemicals in Aquatic Food Webs. *QSAR Comb. Sci.* **2003**, *22*, 337–345. [CrossRef]
5. Grisoni, F.; Consonni, V.; Villa, S.; Vighi, M.; Todeschini, R. QSAR Models for Bioconcentration: Is the Increase in the Complexity Justified by More Accurate Predictions? *Chemosphere* **2015**, *127*, 171–179. [CrossRef]
6. Chmiel, T.; Mieszkowska, A.; Kempińska-Kupczyk, D.; Kot-Wasik, A.; Namieśnik, J.; Mazerska, Z. The Impact of Lipophilicity on Environmental Processes, Drug Delivery and Bioavailability of Food Components. *Microchem. J.* **2019**, *146*, 393–406. [CrossRef]
7. Costanza, J.; Lynch, D.G.; Boethling, R.S.; Arnot, J.A. Use of the Bioaccumulation Factor to Screen Chemicals for Bioaccumulation Potential. *Environ. Toxicol. Chem.* **2012**, *31*, 2261–2268. [CrossRef]
8. Wanat, K. Biological Barriers, and the Influence of Protein Binding on the Passage of Drugs across Them. *Mol. Biol. Rep.* **2020**, *47*, 3221–3231. [CrossRef]
9. Alonso, C.; Carrer, V.; Espinosa, S.; Zanuy, M.; Córdoba, M.; Vidal, B.; Domínguez, M.; Godessart, N.; Coderch, L.; Pont, M. Prediction of the Skin Permeability of Topical Drugs Using In Silico and In Vitro Models. *Eur. J. Pharm. Sci.* **2019**, *136*, 104945. [CrossRef]
10. Bertato, L.; Chirico, N.; Papa, E. Predicting the Bioconcentration Factor in Fish from Molecular Structures. *Toxics* **2022**, *10*, 581. [CrossRef]
11. Valko, K. Application of Biomimetic HPLC to Estimate In Vivo Behavior of Early Drug Discovery Compounds. *Future Drug Discov.* **2019**, *1*, FDD11. [CrossRef]
12. Valko, K.L. Biomimetic Chromatography—A Novel Application of the Chromatographic Principles. *Anal. Sci. Adv.* **2022**, *3*, 146–153. [CrossRef]
13. Russo, G.; Grumetto, L.; Szucs, R.; Barbato, F.; Lynen, F. Determination of In Vitro and In Silico Indexes for the Modeling of Blood-Brain Barrier Partitioning of Drugs via Micellar and Immobilized Artificial Membrane Liquid Chromatography. *J. Med. Chem.* **2017**, *60*, 3739–3754. [CrossRef]
14. Ulenberg, S.; Ciura, K.; Georgiev, P.; Pastewska, M.; Ślifirski, G.; Król, M.; Herold, F.; Bączek, T. Use of Biomimetic Chromatography and In Vitro Assay to Develop Predictive GA-MLR Model for Use in Drug-Property Prediction among Anti-Depressant Drug Candidates. *Microchem. J.* **2022**, *175*, 107183. [CrossRef]
15. Ermondi, G.; Vallaro, M.; Caron, G. Learning How to Use IAM Chromatography for Predicting Permeability. *Eur. J. Pharm. Sci.* **2018**, *114*, 385–390. [CrossRef]
16. Verzele, D.; Lynen, F.; Vrieze, M.D.; Wright, A.G.; Hanna-Brown, M.; Sandra, P. Development of the First Sphingomyelin Biomimetic Stationary Phase for Immobilized Artificial Membrane (IAM) Chromatography. *Chem. Commun.* **2012**, *48*, 1162–1164. [CrossRef]
17. Ciura, K.; Kovačević, S.; Pastewska, M.; Kapica, H.; Kornela, M.; Sawicki, W. Prediction of the Chromatographic Hydrophobicity Index with Immobilized Artificial Membrane Chromatography Using Simple Molecular Descriptors and Artificial Neural Networks. *J. Chromatogr. A* **2021**, *1660*, 462666. [CrossRef]
18. Haginaka, J.; Kanasugi, N. Enantioselectivity of Bovine Serum Albumin-Bonded Columns Produced with Isolated Protein Fragments. II. Characterization of Protein Fragments and Chiral Binding Sites. *J. Chromatogr. A* **1997**, *769*, 215–223. [CrossRef]
19. Kim, H.S.; Wainer, I.W. Rapid Analysis of the Interactions between Drugs and Human Serum Albumin (HSA) Using High-Performance Affinity Chromatography (HPAC). *J. Chromatogr. B* **2008**, *870*, 22–26. [CrossRef]

20. Ishii, T.; Minoda, K.; Bae, M.-J.; Mori, T.; Uekusa, Y.; Ichikawa, T.; Aihara, Y.; Furuta, T.; Wakimoto, T.; Kan, T.; et al. Binding Affinity of Tea Catechins for HSA: Characterization by High-Performance Affinity Chromatography with Immobilized Albumin Column. *Mol. Nutr. Food Res.* **2009**, *54*, 816–822. [CrossRef]
21. Valko, K.; Nunhuck, S.; Bevan, C.; Abraham, M.H.; Reynolds, D.P. Fast Gradient HPLC Method to Determine Compounds Binding to Human Serum Albumin. Relationships with Octanol/Water and Immobilized Artificial Membrane Lipophilicity. *J. Pharm. Sci.* **2003**, *92*, 2236–2248. [CrossRef] [PubMed]
22. Chrysanthakopoulos, M.; Giaginis, C.; Tsantili-Kakoulidou, A. Retention of Structurally Diverse Drugs in Human Serum Albumin Chromatography and Its Potential to Simulate Plasma Protein Binding. *J. Chromatogr. A* **2010**, *1217*, 5761–5768. [CrossRef] [PubMed]
23. Anguizola, J.; Bi, C.; Koke, M.; Jackson, A.; Hage, D.S. On-Column Entrapment of Alpha1-Acid Glycoprotein for Studies of Drug-Protein Binding by High-Performance Affinity Chromatography. *Anal. Bioanal. Chem.* **2016**, *408*, 5745–5756. [CrossRef] [PubMed]
24. Xuan, H.; Hage, D.S. Immobilization of A1-Acid Glycoprotein for Chromatographic Studies of Drug–Protein Binding. *Anal. Biochem.* **2005**, *346*, 300–310. [CrossRef]
25. Filipic, S.; Ruzic, D.; Vucicevic, J.; Nikolic, K.; Agbaba, D. Quantitative Structure-Retention Relationship of Selected Imidazoline Derivatives on A1-Acid Glycoprotein Column. *J. Pharm. Biomed. Anal.* **2016**, *127*, 101–111. [CrossRef]
26. Vallianatou, T.; Tsopelas, F.; Tsantili-Kakoulidou, A. Prediction Models for Brain Distribution of Drugs Based on Biomimetic Chromatographic Data. *Molecules* **2022**, *27*, 3668. [CrossRef]
27. Stergiopoulos, C.; Tsopelas, F.; Valko, K.; Ochsenkühn-Petropoulou, M. The Use of Biomimetic Chromatography to Predict Acute Aquatic Toxicity of Pharmaceutical Compounds. *Toxicol. Environ. Chem.* **2021**, *104*, 1–9. [CrossRef]
28. Andrić, F.; Šegan, S.; Tešić, Ž.; Milojković-Opsenica, D. Chromatographic Methods in Determination of the Soil–Water Partition Coefficient. *J. Liq. Chromatogr. Relat. Technol.* **2016**, *39*, 249–256. [CrossRef]
29. Hidalgo-Rodríguez, M.; Fuguet, E.; Ràfols, C.; Rosés, M. Performance of Chromatographic Systems to Model Soil–Water Sorption. *J. Chromatogr. A* **2012**, *1252*, 136–145. [CrossRef]
30. Sobańska, A.W. Immobilized Artificial Membrane-Chromatographic and Computational Descriptors in Studies of Soil-Water Partition of Environmentally Relevant Compounds. *Env. Sci. Pollut. Res.* **2022**, *30*, 6192–6200. [CrossRef]
31. Sobańska, A.W. Affinity of Compounds for Phosphatydylcholine-Based Immobilized Artificial Membrane—A Measure of Their Bioconcentration in Aquatic Organisms. *Membranes* **2022**, *12*, 1130. [CrossRef]
32. Farsa, O. Chromatographic Behaviour Predicts the Ability of Potential Nootropics to Permeate the Blood-Brain Barrier. *Sci. Pharm.* **2013**, *81*, 81–91. [CrossRef]
33. Grooten, Y.; Mangelings, D.; Van der Heyden, Y. Predicting Skin Permeability of Pharmaceutical and Cosmetic Compounds Using Retention on Octadecyl, Cholesterol-Bonded and Immobilized Artificial Membrane Columns. *J. Chromatogr. A* **2022**, *1676*, 463271. [CrossRef]
34. Turowski, M.; Kaliszan, R. Keratin Immobilized on Silica as a New Stationary Phase for Chromatographic Modelling of Skin Permeation. *J. Pharm. Biomed. Anal.* **1997**, *15*, 1325–1333. [CrossRef]
35. Barbato, F.; Cappello, B.; Miro, A.; La Rotonda, M.; Quaglia, F. Chromatographic Indexes on Immobilized Artificial Membranes for the Prediction of Transdermal Transport of Drugs. *Il Farm.* **1998**, *53*, 661–665. [CrossRef]
36. Hidalgo-Rodríguez, M.; Soriano-Meseguer, S.; Fuguet, E.; Ràfols, C.; Rosés, M. Evaluation of the Suitability of Chromatographic Systems to Predict Human Skin Permeation of Neutral Compounds. *Eur. J. Pharm. Sci.* **2013**, *50*, 557–568. [CrossRef]
37. Jevric, L.R.; Podunavac Kuzmanovic, S.O.; Svarc Gajic, J.V.; Kovacevic, S.; Jovanovic, B.Z. RP-HPTLC Retention Data in Correlation with the In-Silico ADME Properties of a Series of s-Triazine Derivatives. *Iran. J. Pharm. Res.* **2014**, *13*, 1203–1211. [CrossRef]
38. Kovačević, S.; Jevrić, L.R.; Podunavac Kuzmanović, S.O.; Lončar, E.S. Prediction of In Silico ADME Properties of 1,2-O-Isopropylidene Aldohexose Derivatives. *Iran. J. Pharm. Res.* **2014**, *13*, 899–907. [CrossRef]
39. Lazaro, E.; Rafols, C.; Abraham, M.H.; Rosés, M. Chromatographic Estimation of Drug Disposition Properties by Means of Immobilized Artificial Membranes (IAM) and C18 Columns. *J. Med. Chem.* **2006**, *49*, 4861–4870. [CrossRef]
40. Martínez-Pla, J.J.; Martín-Biosca, Y.; Sagrado, S.; Villanueva-Camañas, R.M.; Medina-Hernández, M.J. Evaluation of the pH Effect of Formulations on the Skin Permeability of Drugs by Biopartitioning Micellar Chromatography. *J. Chromatogr. A* **2004**, *1047*, 255–262. [CrossRef]
41. Nasal, A.; Sznitowska, M.; Buciński, A.; Kaliszan, R. Hydrophobicity Parameter from High-Performance Liquid Chromatography on an Immobilized Artificial Membrane Column and Its Relationship to Bioactivity. *J. Chromatogr. A* **1995**, *692*, 83–89. [CrossRef]
42. Naseem, S.; Zushi, Y.; Nabi, D. Development and Evaluationof Two-Parameter Linear Free Energy Models for the Prediction of Human Skin Permeability Coefficient of Neutral Organic Chemicals. *J. Cheminform.* **2021**, *13*, 25. [CrossRef] [PubMed]
43. Soriano-Meseguer, S.; Fuguet, E.; Port, A.; Rosés, M. Estimation of Skin Permeation by Liquid Chromatography. *ADMET DMPK* **2018**, *6*, 140–152. [CrossRef]
44. Wang, Y.; Sun, J.; Liu, H.; Liu, J.; Zhang, L.; Liu, K.; He, Z. Predicting Skin Permeability Using Liposome Electrokinetic Chromatography. *Analyst* **2009**, *134*, 267–272. [CrossRef] [PubMed]
45. Waters, L.J.; Shahzad, Y.; Stephenson, J. Modelling Skin Permeability with Micellar Liquid Chromatography. *Eur. J. Pharm. Sci.* **2013**, *50*, 335–340. [CrossRef]

46. Sobańska, A.W.; Robertson, J.; Brzezińska, E. Application of RP-18 TLC Retention Data to the Prediction of the Transdermal Absorption of Drugs. *Pharmaceuticals* **2021**, *14*, 147. [CrossRef]
47. Ciura, K.; Dziomba, S.; Nowakowska, J.; Markuszewski, M.J. Thin Layer Chromatography in Drug Discovery Process. *J. Chromatogr. A* **2017**, *1520*, 9–20. [CrossRef]
48. Sobańska, A.W.; Brzezińska, E. IAM Chromatographic Models of Skin Permeation. *Molecules* **2022**, *27*, 1893. [CrossRef]
49. Hong, H.; Wang, L.; Han, S.; Zou, G. The Estimation of Bioconcentration Factors of Aromatic Hydrocarbons by High-performance Liquid Chromatography. *Toxicol. Environ. Chem.* **1996**, *56*, 185–191. [CrossRef]
50. Guo, R.; Liang, X.; Chen, J.; Zhang, Q.; Wu, W.; Kettrup, A. Using HPLC Retention Parameters to Estimate Fish Bioconcentration Factors of Organic Compounds. *J. Liq. Chromatogr. Relat. Technol.* **2004**, *27*, 1861–1873. [CrossRef]
51. Sobanska, A. RP-18 TLC Retention Data and Calculated Physico-Chemical Parameters as Predictors of Soil-Water Partition and Bioconcentration of Organic Sunscreens. *Chemosphere* **2021**, *279*, 130527. [CrossRef]
52. Tsopelas, F.; Stergiopoulos, C.; Tsakanika, L.-A.; Ochsenkühn-Petropoulou, M.; Tsantili-Kakoulidou, A. The Use of Immobilized Artificial Membrane Chromatography to Predict Bioconcentration of Pharmaceutical Compounds. *Ecotoxicol. Environ. Saf.* **2017**, *139*, 150–157. [CrossRef]
53. Daina, A.; Michielin, O.; Zoete, V. SwissADME: A Free Web Tool to Evaluate Pharmacokinetics, Drug-Likeness and Medicinal Chemistry Friendliness of Small Molecules. *Sci. Rep.* **2017**, *7*, 42717. [CrossRef]
54. U.S. Environmental Protection Agency. EPISuiteTM-Estimation Program Interface | USEPA. Available online: https://www.epa.gov/tsca-screening-tools/epi-suitetm-estimation-program-interface (accessed on 2 January 2023).
55. Seung, L.J. EPISuite: A Fascinate Predictive Tool for Estimating the Fates of Organic Contaminants. *J. Bioremediat. Biodegrad.* **2016**, *7*, e171. [CrossRef]
56. Stepanov, D.; Canipa, S.; Wolber, G. HuskinDB, a Database for Skin Permeation of Xenobiotics. *Sci. Data* **2020**, *7*, 426. [CrossRef]
57. Lunghini, F.; Marcou, G.; Azam, P.; Patoux, R.; Enrici, M.H.; Bonachera, F.; Horvath, D.; Varnek, A. QSPR Models for Bioconcentration Factor (BCF): Are They Able to Predict Data of Industrial Interest? *SAR QSAR Environ. Res.* **2019**, *30*, 507–524. [CrossRef]
58. Potts, R.O.; Guy, R.H. Predicting Skin Permeability. *Pharm. Res.* **1992**, *9*, 663–669. [CrossRef]
59. Meylan, W.M.; Howard, P.H.; Boethling, R.S.; Aronson, D.; Printup, H.; Gouchie, S. Improved Method for Estimating Bioconcentration/Bioaccumulation Factor from Octanol/Water Partition Coefficient. *Environ. Toxicol. Chem.* **1999**, *18*, 664–672. [CrossRef]
60. Fu, X.C.; Wang, G.P.; Wang, Y.F.; Liang, W.Q.; Yu, Q.S.; Chow, M.S.S. Limitation of Potts and Guy's Model and a Predictive Algorithm for Skin Permeability Including the Effects of Hydrogen-Bond on Diffusivity. *Pharmazie* **2004**, *59*, 282–285.
61. Cronin, M.T.D.; Dearden, J.C.; Moss, G.P.; Murray-Dickson, G. Investigation of the Mechanism of Flux across Human Skin In Vitro by Quantitative Structure–Permeability Relationships. *Eur. J. Pharm. Sci.* **1999**, *7*, 325–330. [CrossRef]
62. Mitragotri, S.; Anissimov, Y.G.; Bunge, A.L.; Frasch, H.F.; Guy, R.H.; Hadgraft, J.; Kasting, G.B.; Lane, M.E.; Roberts, M.S. Mathematical Models of Skin Permeability: An Overview. *Int. J. Pharm.* **2011**, *418*, 115–129. [CrossRef] [PubMed]

Disclaimer/Publisher's Note: The statements, opinions and data contained in all publications are solely those of the individual author(s) and contributor(s) and not of MDPI and/or the editor(s). MDPI and/or the editor(s) disclaim responsibility for any injury to people or property resulting from any ideas, methods, instructions or products referred to in the content.